Dalton Transactions

PAPER

View Article Online
View Journal | View Issue

Cite this: *Dalton Trans.*, 2016, **45**, 8050

Enhanced kinetic stability of $[Pd_2L_4]^{4+}$ cages through ligand substitution†

Dan Preston,[a] Samantha M. McNeill,[b] James E. M. Lewis,[a] Gregory. I. Giles[b] and James D. Crowley*[a]

Received 11th January 2016,
Accepted 5th April 2016

DOI: 10.1039/c6dt00133e

www.rsc.org/dalton

There is considerable interest in exploiting metallosupramolecular cages as drug delivery vectors. Recently, we developed a $[Pd_2L_4]^{4+}$ cage capable of binding two molecules of cisplatin. Unfortunately, this first generation cage was rapidly decomposed by common biologically relevant nucleophiles. In an effort to improve the kinetic stability of these cage architectures here we report the synthesis of two amino substituted tripyridyl 2,6-bis(pyridin-3-ylethynyl)pyridine (**tripy**) ligands (with amino groups either in the 2-(**2A-tripy**) or 3-(**3A-tripy**) positions of the terminal pyridines) and their respective $[Pd_2(\mathbf{L_{tripy}})_4]^{4+}$ cages. These systems have been characterised by ^{1}H, ^{13}C and DOSY NMR spectroscopies, high resolution electrospray mass spectrometry, elemental analysis and, in one case, by X-ray crystallography. It was established, using model palladium(II) N-heterocyclic carbene (NHC) probe complexes, that the amino substituted compounds were stronger donor ligands than the parent system (**2A-tripy** > **3A-tripy** > **tripy**). Competition experiments with a range of nucleophiles showed that these substitutions lead to more kinetically robust cage architectures, with $[Pd_2(\mathbf{2A\text{-}tripy})_4]^{4+}$ proving the most stable. Biological testing on the three ligands and cages against A549 and MDA-MB-231 cell lines showed that only $[Pd_2(\mathbf{2A\text{-}tripy})_4]^{4+}$ exhibited any appreciable cytotoxicity, with a modest IC_{50} of 36.4 ± 1.9 μM against the MDA-MB-231 cell line. Unfortunately, the increase in kinetic stability of the $[Pd_2(\mathbf{L_{tripy}})_4]^{4+}$ cages was accompanied by loss of cisplatin-binding ability.

Introduction

Interest in self-assembled coordination complexes of well-defined two- and three-dimensional geometries, or metallosupramolecular architectures,[1] continues to grow due to their potential in a range of applications. The molecular recognition properties of these systems have been used to develop molecular reactions flasks,[2] catalysts[3] and drug delivery agents.[4] Systems have also been used to sequester reactive species,[5] and environmental pollutants.[6] Additionally, the biological,[7] photophysical,[8] electronic[9] and redox[10] properties of these metallosupramolecular architectures have been studied.

As part of our interest in the biological properties[11] of metallosupramolecular architectures we have previously reported the synthesis of a tripyridyl (**tripy**) $[Pd_2L_4]^{4+}$ cage capable of binding cisplatin (*cis*-$[Pt(NH_3)_2Cl_2]$).[11d] We hoped to exploit these $[Pd_2L_4]^{4+}$ cages as metallosupramolecular drug delivery vectors, unfortunately the cage architecture was rapidly decomposed when exposed to chloride (Cl^-),[11a,d,12] histidine (*his*)[11a] and cysteine (*cys*)[11a] (common nucleophiles in biological systems). In order to use these cisplatin binding $[Pd_2L_4]^{4+}$ cages as drug delivery agents a method for increasing the kinetic stability of these metallosupramolecular architectures against nucleophiles was required.[13] There are two obvious approaches to enhance the kinetic stability of the cage architectures: (1) assemble the cage using more kinetically inert metal ions or (2) sterically and electronically tune the **tripy** ligand framework. Exploiting kinetically inert metals for the generation of metallosupramolecular architectures can be difficult due to the formation of kinetically "trapped" intermediate structures that cannot "error-correct" into the desired system. Therefore we chose to generate more electron-donating tripyridyl ligands in an effort to obtain more kinetically robust $[Pd_2L_4]^{4+}$ cages. Herein we report the synthesis of two new amino substituted tripyridyl ligands (**2A-tripy** and **3A-tripy**) and their respective cages (Scheme 1). The addition of the amino groups to the 2- and 3-positions of the terminal ligating pyridyl units of the ligand framework was expected to increase the donor properties of the ligands and lead to more kineti-

[a]*Department of Chemistry, University of Otago, PO Box 56, Dunedin, New Zealand. E-mail: jcrowley@chemistry.otago.ac.nz*
[b]*Department of Pharmacology and Toxicology, University of Otago, PO Box 56, Dunedin, New Zealand*

†Electronic supplementary information (ESI) available: The experimental procedures, ^{1}H, ^{13}C and DOSY NMR, HR-ESMS, crystallographic and computational data. CCDC 1439952. For ESI and crystallographic data in CIF or other electronic format see DOI: 10.1039/c6dt00133e

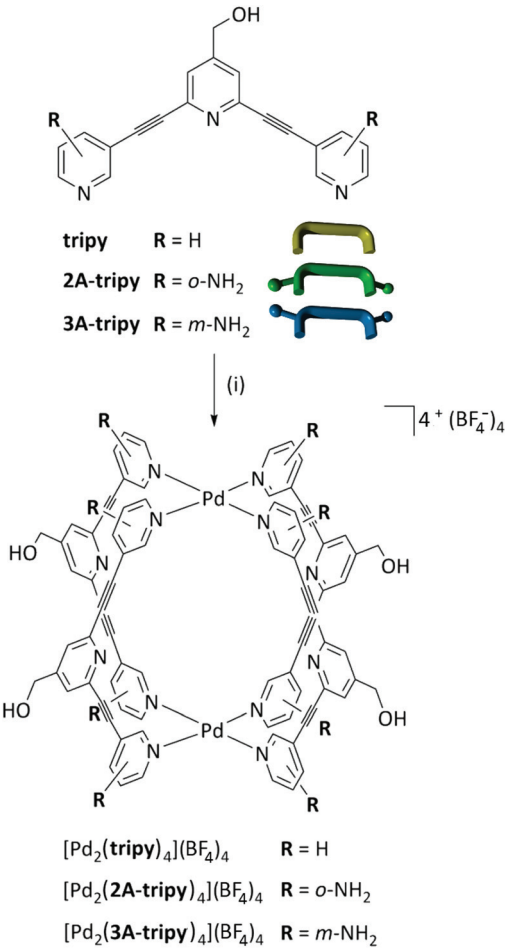

Scheme 1 Synthesis of the $[Pd_2(L_{tripy})_4]^{4+}$ cages from the tripyridyl ligands (**tripy**, **2A-tripy**, **3A-tripy**). Conditions: (i) $[Pd(CH_3CN)_4](BF_4)_2$, solvent (CH_3CN, DMF or DMSO), RT or 50 °C.

cally robust cage architectures. Additionally, the presence of the 2-amino units within the $[Pd_2(\mathbf{2A\text{-}tripy})_4]^{4+}$ cage architecture was expected to sterically reduce access to the palladium(II) ions potentially further enhancing the cage lifetime in the presence of biological nucleophiles. Competition experiments with Cl^-, *his* and *cys* nucleophiles showed that the $[Pd_2(\mathbf{2A\text{-}tripy})_4]^{4+}$ cage was more stable than the $[Pd_2(\mathbf{3A\text{-}tripy})_4]^{4+}$ cage which in turn was more stable than the $[Pd_2(\mathbf{tripy})_4]^{4+}$ cage. Unfortunately, the structural and electronic changes imposed through amino substitution in the 2-position circumscribe the ability of the cage to encapsulate cisplatin. Preliminary biological testing on these systems indicated that only $[Pd_2(\mathbf{2A\text{-}tripy})_4]^{4+}$ exhibited an IC_{50} < 50 μM against either of the two investigated cell lines.

Results and discussion

Synthesis and characterisation

The electronically and sterically tuned tripyridyl ligands (**tripy**, **2A-tripy**, and **3A-tripy**, Scheme 1) were synthesised using standard methods[11d,12,14] (ESI†) and characterised using NMR spectroscopy, high resolution electrospray mass spectrometry (HR-ESMS), and elemental analysis (Experimental section and ESI†).

Addition of one of the ligands (**tripy**, **2A-tripy**, and **3A-tripy**) to a solution of $[Pd(CH_3CN)_4](BF_4)_2$ in a 2 : 1 ratio resulted in the formation of the desired cages (Scheme 1). While the **tripy** and **3A-tripy** containing cages formed instantaneously at room temperature, the formation of $[Pd_2(\mathbf{2A\text{-}tripy})_4](BF_4)_4$ required heating in DMSO solution at 50 °C for six hours to complete the assembly. The cages were characterised using ^1H and DOSY NMR spectroscopy, HR-ESMS, and elemental analysis, (Experimental and ESI†). The ^1H NMR spectra (Fig. 1 and ESI†) of the $[Pd_2(L_{tripy})_4]^{4+}$ cages show a single set of peaks. The proton resonances due to the terminal pyridyl units of the cages (H_{c-f}) are shifted downfield ($\Delta\delta$ = 0.19–0.59 ppm) relative to the free **tripy** ligands, consistent with complexation to palladium(II) ions. Interestingly, the proton resonance of the 2-amino group in the $[Pd_2(\mathbf{2A\text{-}tripy})_4](BF_4)_4$ cage displays a very large ($\Delta\delta(H_{NH})$ = 1.56 ppm) shift relative to the free ligand (Fig. 1). Presumably, this large shift is caused by a combination of coordination to the palladium(II) ions and intra-ligand hydrogen bonding interactions between the amino groups on the adjacent ligands. Consistent with this postulate, the shift of the corresponding proton resonance in the $[Pd_2(\mathbf{3A\text{-}tripy})_4](BF_4)_4$ cage is much smaller ($\Delta\delta(H_{NH})$ = 0.81 ppm, ESI†). The sharp, uncomplicated signals observed in the ^1H NMR spectra of the $[Pd_2(L_{tripy})_4]^{4+}$ systems are similar to what was previously observed for the formation of other $[Pd_2(L)_4]^{4+}$ cages and are consistent with the formation of complexes of high symmetry in solution.[11a,d,12]

Diffusion-ordered ^1H NMR spectroscopy (DOSY) provided additional strong support for the selective formation of the cages in solution. ^1H DOSY spectra (d_6-DMSO, 298 K) were obtained for ligands (**tripy**, **2A-tripy**, and **3A-tripy**) and cages ($[Pd_2(\mathbf{tripy})_4]^{4+}$, $[Pd_2(\mathbf{2A\text{-}tripy})_4]^{4+}$ and $[Pd_2(\mathbf{3A\text{-}tripy})_4]^{4+}$ (ESI†)). Each of the proton signals in the individual spectra show the same diffusion coefficient (D), indicating that there is only one species present in solution (ESI†). The $D_{complex}/D_{ligand}$ ratios of ~0.50 : 1 are similar to those observed for related literature

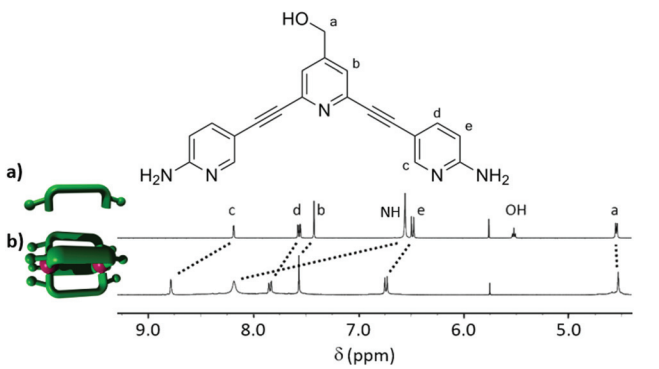

Fig. 1 Partial ^1H NMR spectra (298 K, 500 MHz, d_6-DMSO) of (a) **2A-tripy** and (b) the cage $[Pd_2(\mathbf{2A\text{-}tripy})_4](BF_4)_4$.

compounds[11a,d,12] and suggest that the palladium(II) cage species are stable in solution (ESI†).

Mass spectra (HR-ESMS) of the $[Pd_2(\mathbf{L_{tripy}})_4]^{4+}$ cage systems in DMF–CH_3CN solution obtained under pseudo cold-spray conditions displayed overlapping peaks due to $[Pd_2L_4]^{4+}$ and $[PdL_2]^{2+}$ ions. Additionally, the spectrum of the **3A-tripy** based cage displayed a peak due to the $[Pd_2(\mathbf{3A\text{-}tripy})_4(BF_4)_2]^{2+}$ ion.

After considerable effort (>50 crystallisations and data collections) the solid state structure of the $[Pd_2(\mathbf{2A\text{-}tripy})_4](BF_4)_4$ complex was obtained using X-ray crystallography (Fig. 2 and ESI†). Small weakly diffracting X-ray quality crystals were generated by vapour diffusion of diethyl ether into a CH_3CN solution of the $[Pd_2(\mathbf{2A\text{-}tripy})_4](BF_4)_4$ cage. Although the weak diffraction was, at least in part, due to the presence of multiple disordered solvent molecules and counter anions within the crystal lattice (*vide infra*), the cationic framework of the cage was readily identified (Fig. 2).

The solid state structure of the $[Pd_2(\mathbf{2A\text{-}tripy})_4]^{4+}$ cage confirms that the coordination of the 2-amino pyridyl units to the palladium(II) ions was monodentate through the pyridyl nitrogen as expected.[15] Additionally, the 2-amino units of the ligands are engaged in intra-ligand hydrogen bonding interactions (N···N 3.78(3) Å, N–H···N 2.94 Å, Fig. 2b and ESI†) consistent with ^{1}H NMR data described above. In contrast to the $[Pd_2(\mathbf{tripy})_4]^{4+}$ cage,[16] the $[Pd_2(\mathbf{2A\text{-}tripy})_4]^{4+}$ cation adopts a more twisted structure in which the ligands of the **2A-tripy** cages are significantly bent out of planarity and this appears to be caused by hydrogen bonding interactions between the amino groups on the *exo* faces of the architecture. This is quite different to what has been previously observed in the solid state structures of unsubstituted $[Pd_2(\mathbf{tripy})_4]^{4+}$ cations, these cages without the 2-amino groups all were found to adopt a lantern shape, with essentially planar tripy ligands.[11a,d,12] The coordinated **2A-tripy** ligand distorts in two ways: a swivelling of the coordinating pyridine rings relative to the principal rotation axis of the molecule (θ = 34.44°–34.64°, compared with θ = 3.47°–9.42° for $[Pd_2(\mathbf{tripy})_4]^{4+}$) and a twisting of the central pyridine out of the plane through which the ligand coordinates to the two Pd(II) centres (φ = 35.10° compared with φ = 5.61° for $[Pd_2(\mathbf{tripy})_4]^{4+}$). The cavity dimensions also differ (a Pd···Pd distance of 11.530(9)–11.610(9) Å compared with 11.201(1) Å for $[Pd_2(\mathbf{tripy})_4]^{4+}$, and a core-to-core pyridyl N···N distance of 10.711(9)–10.732(9) Å compared with 11.07(1)–11.26(1) Å for $[Pd_2(\mathbf{tripy})_4]^{4+}$, Table 1).

Interestingly, the central cavity of the $[Pd_2(\mathbf{2A\text{-}tripy})_4]^{4+}$ cage is filled in the solid state. The *exo*-methylene alcohol (CH_2OH) substituents from the four neighbouring cages in the crystal lattice penetrate into the cavity of each cage and form a hydrogen bonding interaction (O···N 2.74(3) Å, O–H···N 1.91 Å, Fig. 3 and ESI†) with the *endo*-pyridyl unit. These interactions generate 2D supramolecular sheets of cages through the solid state structure (Fig. 3 and ESI†).

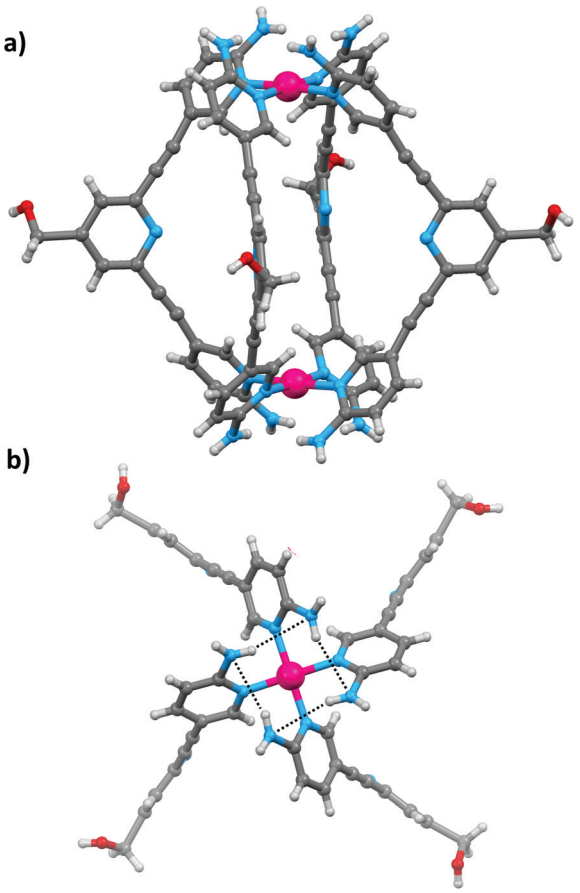

Fig. 2 Molecular structure of $[Pd_2(\mathbf{2A\text{-}tripy})_4]^{4+}$ cations determined using X-ray crystallography: (a) a ball-and-stick representation of $[Pd_2(\mathbf{2A\text{-}tripy})_4]^{4+}$ cation; (b) a partial view of the $[Pd_2(\mathbf{2A\text{-}tripy})_4]^{4+}$ cation from the top showing the hydrogen bonding interactions between the 2-amino substituents of the ligands. Solvent molecules and counterions omitted for clarity. Colours: magenta = palladium, grey = carbon, white = hydrogen, blue = nitrogen, red = oxygen.

Competition experiments, cisplatin binding and cytotoxicity studies

The relative pK_a values of 2-aminopyridine (6.82), 3-aminopyridine (6.04), and pyridine (5.23) indicate that 2-aminopyridine is the most basic ligand.[17] Evidence that 2-aminopyridine was also the strongest nucleophile was obtained using the palladium(II)-N-heterocyclic carbene (NHC) probe system developed by Huynh and coworkers (Table 2 and ESI†).[18] Consistent with the pK_a values, the probe complexes indicated that 2-aminopyridine (161.2 ppm) is a stronger donor than 3-aminopyridine (159.8 ppm) which is a stronger donor than pyridine (159.3 ppm). The chemical shift observed for the 2-aminopyridine ligand is very similar to that previously reported for *N*-methylimidazole (161.1 ppm)[18b] suggesting that the donor strength of these ligands are similar. To allow direct comparison to the literature pK_a values (Table 2) and for synthetic convenience[11a] we have examined the probe complexes of the simpler pyridine rather than the tripyridyl ligands. However, these pyridine model systems can serve as proxies for their respective tripyridyl ligands (**2A-tripy**, **3A-tripy**, **tripy**) and provide indirect experimental evidence for the donor properties of the tripy ligands because the steric and electronic changes on going from the pyridine to tripy ligands are the

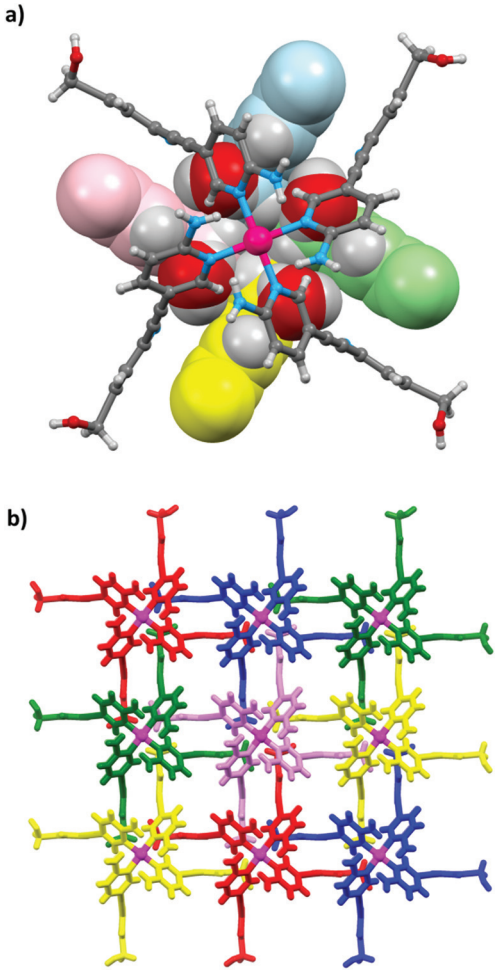

Fig. 3 The crystal packing of $[Pd_2(\mathbf{2A\text{-}tripy})_4]^{4+}$ cations showing (a) the interdigitation of the methylene alcohol substituents on adjacent $[Pd_2(\mathbf{2A\text{-}tripy})_4]^{4+}$ cations into the central cavity of the $[Pd_2(\mathbf{2A\text{-}tripy})_4]^{4+}$ cation (cage shown in ball-and-stick, methylene alcohol substituents in spacefilling view), and (b) the extended lattice.

Table 1 Selected crystallographic distances and angles from $[Pd_2(\mathbf{2A\text{-}tripy})_4]^{4+}$ and $[Pd_2(\mathbf{tripy})_4]^{4+}$ [16]

	$[Pd_2(\mathbf{2A\text{-}tripy})_4]^{4+}$	$[Pd_2(\mathbf{tripy})_4]^{4+}$ [16]
Θ (°)[a]	34.44°–34.64°	3.47°–9.42°
Φ (°)[b]	35.10°	5.61°
d(Pd(II)···Pd(II)) (Å)	11.53(9)–11.610(9) Å	11.201(1) Å
d(N_{core}···N_{core}) (Å)	10.71(9)–10.73(9) Å	11.07(1)–11.26(1) Å

[a] θ: the swivelling of the coordinating pyridine rings relative to the principal rotation axis of the molecule. [b] φ: twisting of the central pyridine out of the plane through which the ligand coordinates to the two Pd(II) centres.

same across the series. Thus the model complexes provide a qualitative ranking of the substituents' effects present in the tripy ligands and strongly suggest that the donor properties of the tripyridyl ligands follow the order **2A-tripy** > **3A-tripy** > **tripy**.

Table 2 pK_a values, ^{13}C NMR chemical shifts of NHC carbene of the model probe complexes, and half-lives ($t_{1/2}$) for the decomposition of the $[Pd_2(L_{tripy})_4]^{4+}$ architectures against selected biologically relevant nucleophiles (3 : 2 d_6-DMSO/D_2O, 298 K, 500 MHz) as measured through time-course ^{1}H NMR spectroscopy

Compound	pK_a	^{13}C δ^a (ppm)	Cl^- (8 eq.)	*his* (4 eq.)	*cys* (4 eq.)
$[Pd_2(\mathbf{tripy})_4](BF_4)_4$	5.23[17]	159.3[a,18]	>1 min	18 min	6 min
$[Pd_2(\mathbf{2A\text{-}tripy})_4](BF_4)_4$	6.82[17]	161.2[a]	2 h	46 h	3 h
$[Pd_2(\mathbf{3A\text{-}tripy})_4](BF_4)_4$	6.04[17]	159.8[a]	10 min	25 min	10 min

[a] Chemical shift (ppm) of the NHC carbene carbon in the model Pd(II) probe complexes (ESI).

The kinetic stability of the $[Pd_2(\mathbf{L_{tripy}})_4]^{4+}$ architectures in the presence of common biological nucleophiles (Cl^-, *his* and *cys*) was determined using ^{1}H NMR competition experiments (Table 2 and ESI†). Time-course ^{1}H NMR competition experiments were carried out in 3 : 2 d_6-DMSO/D_2O where 3 mM solutions of each cage were treated with 8 equivalents of tetramethylammonium chloride or 4 equivalents of *his* or *cys*. Under these conditions the unsubstituted $[Pd_2(\mathbf{tripy})_4]^{4+}$ cage was rapidly decomposed by all the nucleophiles. The half-life for the decomposition of the $[Pd_2(\mathbf{tripy})_4]^{4+}$ complex with *his* was 18 minutes. Despite the $[Pd_2(\mathbf{3A\text{-}tripy})_4]^{4+}$ architecture containing the slightly more electron rich **3A-tripy** ligand the cage was still quickly decomposed by each of the nucleophiles. However, the $t_{1/2}$ were subtly increased against all the nucleophiles (for *his* $t_{1/2}$ = 25 min) suggesting that the enhanced ligand donor properties of the **3A-tripy** ligand does lead to increased cage stability relative to the unsubstituted system.

The $[Pd_2(\mathbf{2A\text{-}tripy})_4]^{4+}$ cage displayed markedly higher stability against all the nucleophiles studied. The half-lives for the **2A-tripy** cage decomposition against each nucleophile were all over 2 h, whereas the corresponding $t_{1/2}$ for the other cages were all less than 30 min. **2A-tripy** is only a modestly stronger donor ligand than the **3A-tripy**, and thus the observed large difference in stability is presumably not predominantly due to the increase donor ability of the ligand. A more important element is likely to be the presence of the 2-amino groups on the *exo*-faces of the $[Pd_2(\mathbf{2A\text{-}tripy})_4]^{4+}$ cage which sterically protect the palladium(II) ions from the incoming nucleophiles. Additionally, as observed in the X-ray structure (Fig. 3), the hydrogen bonding interactions between the eight amino groups of the four **2A-tripy** ligands may further enhance the stability of the $[Pd_2(\mathbf{2A\text{-}tripy})_4]^{4+}$ cage relative to the other **tripy** architectures. However, against the stronger nucleophiles (Cl^- and *cys*) the half-lives for the decomposition of the $[Pd_2(\mathbf{2A\text{-}tripy})_4]^{4+}$ are less than 3 h suggesting that these systems would need further tuning in order to be useful in a biological setting.

Cisplatin binding

We[11d,12,19] and others[16] have previously shown that other similar $[Pd_2(\mathbf{tripy})_4]^{4+}$ cages can encapsulate cisplatin through hydrogen bonding interactions in CH_3CN and DMF solvents.[20]

^{1}H NMR spectroscopy and recently reported crystallographic evidence[16b] confirms that despite the presence of the potential hydrogen bond donor CH_2OH units of the *exo* surface of the $[Pd_2(\mathbf{tripy})_4]^{4+}$ cage the system retains the ability to bind cisplatin. Addition of an excess of cisplatin to a d_7-DMF solution of $[Pd_2(\mathbf{tripy})_4]^{4+}$ resulted in a large downfield shift ($\Delta\delta$ = 0.24 ppm) of the internally directed cage proton H_c (Fig. 4a and b) indicative of cisplatin binding within the cage cavity. The solid state structure[16b] of the $[(\text{cisplatin})_2\subset Pd_2(\mathbf{tripy})_4]^{4+}$ host–guest adduct has recently been reported by Casini, Kuhn and co-workers and is very similar to what we have previously observed in related systems.[11d,19b] Consistent with the ^{1}H NMR evidence, the $[Pd_2(\mathbf{tripy})_4]^{4+}$ cation binds two molecules of cisplatin within the cavity of the cage.[16] The guest molecules are rotated 180° with respect to each other; hydrogen bonds between the guests and cage (N–H···N_{Py} and Cl···H–C_{Py}) as well as a metal–metal interaction between the platinum atoms of the guests were observed (Fig. 3a).[11d,16b,19b]

A similar ^{1}H NMR experiment with cisplatin and $[Pd_2(\mathbf{3A\text{-}tripy})_4]^{4+}$ indicated that the 3-amino substituted cage is also able to bind cisplatin in solution, albeit more weakly ($\Delta\delta$ = 0.07 ppm for H_c, Fig. 4c and d) than the parent $[Pd_2(\mathbf{tripy})_4]^{4+}$ cage. Conversely, ^{1}H NMR spectra of the $[Pd_2(\mathbf{2A\text{-}tripy})_4]^{4+}$ cage in the presence of cisplatin acquired in either deuterated CH_3CN or DMF solvents displayed no shifts relative to the free cage indicating that the 2-amino substituted cage is not able to bind cisplatin. We have previously shown that cisplatin binding is very weak[12] and that subtle changes to the size, steric profile and electronic properties of the cage cavity[21] are enough to completely turn off cisplatin binding. Presumably, the lack of cisplatin binding in this system can be ascribed to two factors. Firstly, the presence of the eight amino groups on the *exo* faces of the cage has caused a twisting of the architecture (as indicated in the crystal structure, Fig. 3, and discussed and listed in Table 1). This twisting subtly alters both the size of the cisplatin binding cavity and the orientations of the hydrogen-bond acceptors and donors groups within the cage cavity, weakening the interaction between the host and the cisplatin guest. Secondly, the electron donating 2-amino units push electron density back onto the terminal pyridyl rings of the **tripy** ligand. This would reduce the polarisation of the acidic H_c protons of the pyridyl unit, weakening the hydrogen bonding interaction with chloride ligands of the cisplatin guest. These effects, in concert, appear to be enough to fully circumscribe the already weak cisplatin–cage interaction.[22]

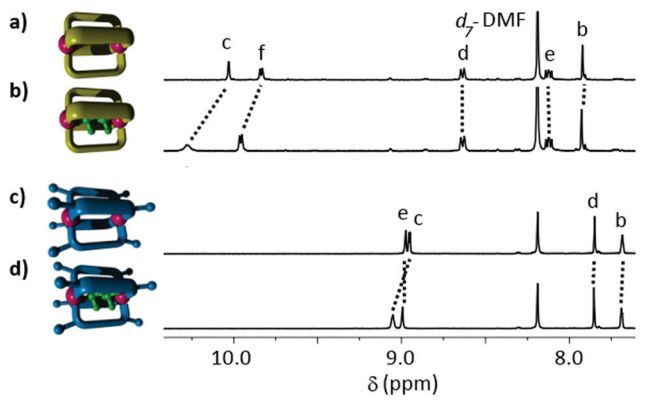

Fig. 4 Partial ^{1}H NMR spectra (298 K, 500 MHz, d_7-DMF) of (a) $[Pd_2(\mathbf{tripy})_4](BF_4)_4$, (b) $[(\text{cisplatin})_2\subset Pd_2(\mathbf{tripy})_4](BF_4)_4$ and (c) $[Pd_2(\mathbf{3A\text{-}tripy})_4](BF_4)_4$ and (d) $[(\text{cisplatin})_2\subset Pd_2(\mathbf{3A\text{-}tripy})_4](BF_4)_4$.

Cytotoxicity

While the improvement of kinetic stability of the $[Pd_2(\mathbf{2A\text{-}tripy})_4]^{4+}$ cage has been achieved at the expense of host–guest capacity, recent work has shown that $[Pd_2(\mathbf{L})_4]^{4+}$ architectures can act as biological agents in their own right.[11a,23] Accordingly, a preliminary investigation of the cytotoxic properties of the three cages (and the corresponding ligands) was undertaken against two cell lines: A549 (lung cancer) and cisplatin-resistant MDA-MB-231 (breast cancer) (Table 3). We have previously determined the IC_{50} values for cisplatin against these two cell lines, which were 9.4 ± 0.3 μM (A549)[24] and 41.2 ± 3.9 μM) (MDA-MB-231)[11b] respectively. None of the ligands exhibited significant cytotoxicity (IC_{50} > 200 μM) against these cell-lines. Similarly, neither of the unstabilised cages, $[Pd_2(\mathbf{tripy})_4](BF_4)_4$ or $[Pd_2(\mathbf{3A\text{-}tripy})_4](BF_4)_4$ (IC_{50} > 50 μM) nor the palladium(II) tetrafluoroborate salt (IC_{50} > 100 μM))[11a] $[Pd(CH_3CN)_4](BF_4)_4$ displayed any appreciable cytotoxic effect. The most kinetically stable cage $[Pd_2(\mathbf{2A\text{-}tripy})_4](BF_4)_4$ displayed low cytotoxicity against the A549 cell line (IC_{50} > 50 μM), and slightly higher cytotoxicity against the

Table 3 IC_{50} values for $[Pd_2(L_{tripy})_4]^{4+}$ and related literature $[Pd_2(L)_4]^{4+}$ compounds against selected cell lines

	IC_{50} (μM)							
	A549 (lung)		MDA-MB231 (breast)		HL-60 (leukemia)		SKW-3 (leukemia)	
Compound	Ligand	Cage	Ligand	Cage	Ligand	Cage	Ligand	Cage
$[Pd_2(\mathbf{tripy})_4](BF_4)_4$	>200	>50	>200	>50	—	—	—	—
$[Pd_2(\mathbf{2A\text{-}tripy})_4](BF_4)_4$	>200	>50	>200	36.4 ± 1.9	—	—	—	—
$[Pd_2(\mathbf{3A\text{-}tripy})_4](BF_4)_4$	>200	>50	>200	>50	—	—	—	—
$[Pd_2(\mathbf{L_a})_4](BF_4)_4$ ($\mathbf{L_a}$ = hextrz)[11a]	28.5 ± 2.6	6.9 ± 0.9	89.8 ± 10.7	6.0 ± 0.6	—	—	—	—
$[Pd_2(\mathbf{L_b})_4](BF_4)_4$ ($\mathbf{L_b}$ = dipy-dianthracenyl)[23]	—	—	—	—	>100	1.9 ± 0.2	>80	1.8 ± 0.2
Cisplatin	—	9.4 ± 0.3	—	41.2 ± 3.9	—	8.1 ± 1.4	—	9.3 ± 2.1

MDA-MB-231 cell line (IC_{50} = 36.4 ± 1.9 μM). We have previously shown that a more kinetically robust and hydrophobic $[Pd_2(\mathbf{L_a})_4]^{4+}$ helicate ($\mathbf{L_a}$ = 1,3-bis(1-hexyl-1*H*-1,2,3-triazol-4-yl) benzene) was considerably more cytotoxic (IC_{50} = 6.9 ± 0.9 and 6.0 ± 0.6 μM) against both the A549 and MDA-MB-231 cell lines.[11a] Additionally, Yoshizawa and co-workers have recently reported that a hydrophobic $[Pd_2(\mathbf{L_b})_4]^{4+}$ cage ($\mathbf{L_b}$ = 3,3′-((4,5,6-tris(2-methoxyethoxy)-1,3-phenylene)bis(anthracene-10,9-diyl))-dipyridine) is highly cytotoxic (IC_{50} = 1.8 and 1.9 μM) against HL-60 and SKW-3 cancer cell lines.[23] Thus it is presumed that low cytotoxicity of the systems described here is connected to the combination of both high kinetic lability and the more hydrophilic nature of the $[Pd_2(\mathbf{L_{tripy}})_4]^{4+}$architectures and ligands.

Conclusions

Two amino substituted tripyridyl 2,6-bis(pyridin-3-ylethynyl) pyridine (**tripy**) ligands (with amino groups either in the 2-(**2A-tripy**) or 3-(**3A-tripy**) positions of the terminal pyridines) and their respective $[Pd_2(\mathbf{L_{tripy}})_4]^{4+}$ cages were synthesised. These systems have been characterised by ^{1}H, ^{13}C and DOSY NMR spectroscopies, high resolution electrospray mass spectrometry, elemental analysis and, in one case, by X-ray crystallography. It was established, using palladium(II) NHC carbene probe model complexes, that the amino substituted compounds were moderately stronger donor ligands than the parent pyridyl system (**2A-tripy** > **3A-tripy** > **tripy**). Competition experiments with common biological nucleophiles (Cl^-, *his* and *cys*) showed that the $[Pd_2(\mathbf{2A\text{-}tripy})_4]^{4+}$ cage proved the most kinetically stable, presumably due to a favourable combination of enhanced ligand donor strength, and probably more importantly, intramolecular hydrogen bonding and steric shielding. Preliminary biological investigations against two cell lines (A549 and MDA-MB-231) found that all ligands and cages had IC_{50} values >50 μM, with the exception of $[Pd_2(\mathbf{2A\text{-}tripy})_4]^{4+}$ which against MDA-MB-231 has an IC_{50} of 36.4 ± 1.9 μM.

However, while the ligand tuning resulted in more robust $[Pd_2(\mathbf{L_{tripy}})_4]^{4+}$ architectures the half-lives of the systems against the stronger nucleophiles were still modest ($t_{1/2}$ = 2–3 h). Furthermore, the subtle structural changes in the most stabilised cage, $[Pd_2(\mathbf{2A\text{-}tripy})_4]^{4+}$ were found to completely destroy the ability of the system to bind cisplatin. Thus, it appears that in order to exploit these types of metallosupramolecular cage architectures as drug delivery vectors, systems assembled from more kinetically inert metals ions such as Pt(II)[4h] and Ru(II)[4e–g] and Co(III)[25] will be required. Efforts to generate more robust systems, composed of kinetically inert metal ions, capable of binding drug molecules are underway.

Experimental

General

Unless otherwise stated, all reagents were purchased from commercial sources and used without further purification. 2,5-Dibromo-4-(hydroxymethyl)pyridine,[26] 5-iodo-2-aminopyridine,[6a] the dimeric dibromobis(benzimidazolin-2-ylidene)dipalladium(II) complex,[27] and *trans*-dibromo(1,3-diisopropylbenzimidazolin-2-ylidene)(pyridine)palladium(II)[18b] were synthesised according to literature procedures. Solvents were laboratory reagent grade. Petroleum ether refers to the fraction of petrol boiling in the range 40–60 °C, isopropyl alcohol (IPA), methanol (CH_3OH), dichloromethane (CH_2Cl_2), ethylenediaminetetraacetate (EDTA), ethynyltrimethylsilane (TMS-acetylene), tetrahydrofuran (THF), dimethyl sulfoxide (DMSO), dimethylformamide (DMF). ^{1}H and ^{13}C NMR spectra were recorded on either a 400 MHz Varian 400-MR or Varian 500 MHz AR spectrometer. Chemical shifts are reported in parts per million and referenced to residual solvent peaks ($CDCl_3$: ^{1}H δ 7.26 ppm, ^{13}C δ 77.16 ppm; CD_3CN: ^{1}H δ 1.94, ^{13}C δ 1.32, 118.26 ppm, d_6-DMSO: ^{1}H δ 2.50 ppm; ^{13}C δ 39.52 ppm). Coupling constants (J) are reported in Hertz (Hz). Standard abbreviations indicating multiplicity were used as follows: m = multiplet, q = quartet, t = triplet, dt = double triplet, d = doublet, dd = double doublet, s = singlet, br = broad. Full ^{1}H and ^{13}C NMR spectra, together with structural labelling are included in the ESI.† IR spectra were recorded on a Bruker ALPHA FT-IR spectrometer with an attached ALPHA-P measurement module. Microanalyses were performed at the Campbell Microanalytical Laboratory at the University of Otago. Electrospray mass spectra (ESMS) were collected on a Bruker microTOF-Q spectrometer.

Synthesis of 5-iodopyridin-2-acetamide (1). A solution of 5-iodopyridin-2-amine (2.5 g, 11.4 mmol) in triethylamine (10 mL) and CH_2Cl_2 (50 mL) was degassed with N_2 for 15 minutes. Acetic anhydride (10.7 mL, 110 mmol) was added and the mixture was stirred at room temperature for 18 hours. After removal of solvents under vacuum, the crude mixture was dissolved in 3 : 1 $CHCl_3$/IPA (150 mL), and washed with saturated aqueous $NaHCO_3$ solution (2 × 75 mL), and brine (75 mL). The organic layer was dried over $MgSO_4$, filtered and the solvent removed under vacuum. Column chromatography on silica (1 : 19 acetone/CH_2Cl_2) gave the product as a brown solid (2.3 g, 8.8 mmol, 77%). ^{1}H NMR (400 MHz, d_6-DMSO, 298 K) δ: 10.58 (1H, s, H_{NH}), 8.50 (1H, d, J = 2.3 Hz, H_a), 8.07 (1H, d, J = 8.8 Hz, H_b), 7.94 (1H, d, J = 8.8 Hz, H_c), 2.08 (3H, s, H_d). ^{13}C NMR (100 MHz, d_6-DMSO, 298 K) δ: 169.4, 153.3 (C_a), 151.2, 145.8 (C_b), 115.3 (C_c), 85.7, 23.9 (C_d). HR ESI-MS ($CHCl_3$) m/z = 284.95 $[M + Na]^+$ (calc. For $C_7H_7IN_2NaO$, 284.95). IR: ν (cm^{-1}) 3215, 3139, 3079, 3018, 1676, 1660, 1520, 1362, 1298, 829, 799. Anal. calcd for: $C_7H_7IN_2O$: C, 32.08; H, 2.69; N, 10.69%. Found: C, 32.30; H, 2.55; N, 10.71%.

Synthesis of *N*-(5-((trimethylsilyl)ethynyl)pyridin-2-yl)acetamide (2). A round bottom flask containing **1** (1.00 g, 3.82 mmol), CuI (0.07 g, 0.38 mmol) and $Pd(PPh_3)_2Cl_2$ (0.19 g, 0.27 mmol) was purged with N_2. Triethylamine (20 mL) was added *via* syringe and the solution was degassed with N_2 for 15 minutes. After adding TMS-acetylene (0.68 g, 0.93 mL, 6.87 mmol) *via* syringe, the reaction was heated at reflux under N_2 for 48 hours. The solvent was removed under vacuum, and the resulting solid was taken up in 3 : 1 $CHCl_3$/IPA (40 mL).

The solution was stirred with aqueous 0.1 M EDTA/NH_4OH solution (40 mL) for 1.5 hours. After washing with aqueous 0.1 M EDTA/NH_4OH (50 mL) and brine (100 mL), the organic layer was dried with Na_2SO_4, filtered, and the solvent removed under vacuum. The solid was purified through column chromatography on silica (1 : 19 acetone/CH_2Cl_2), giving the product as a brown solid (0.86 g, 3.72 mmol, 97%). ^{1}H NMR (500 MHz, $CDCl_3$, 298 K) δ: 8.34 (1H, d, J = 1.6 Hz, H_d), 8.17 (1H, d, J = 8.7 Hz, H_b), 8.07 (1H, br, H_{NH}), 7.77 (1H, dd, J = 8.7 Hz, 2.1 Hz, H_c), 2.21 (3H, s, H_a), 0.25 (15H, s, H_e). ^{13}C NMR (125 MHz, $CDCl_3$, 298 K) δ: 168.5, 150.9 (C_d), 150.3, 141.4 (C_c), 116.0, 112.9 (C_b), 101.4, 97.1, 24.8 (C_a), −0.1 (C_e). HR ESI-MS ($CHCl_3$) m/z = 255.09 $[M + Na]^+$ (calc. for $C_{12}H_{16}N_2NaOSi$, 255.09). IR: ν (cm^{-1}) 3243, 2955, 2161, 1697, 1579, 1526, 1380, 1303, 1246, 1030. Anal. calcd for $C_{12}H_{16}N_2OSi$·0.5 acetone: C, 62.03; H, 7.14; N, 11.35%. Found: C, 61.94; H, 7.29; N, 11.35%.

Synthesis of 5-ethynylpyridin-2-amine (3). A solution of **2** (0.63 g, 2.70 mmol) and NaOH (1.08 g, 27.0 mmol) in methanol (30 mL) was heated at reflux for 1.5 hours before removal of solvent under vacuum, with the resultant residue taken up in 3 : 1 $CHCl_3$/IPA (100 mL) and washed with water (100 mL) and brine (100 mL). After drying with Na_2SO_4 and filtration, the solvent was removed under vacuum, and purification through column chromatography on silica (1 : 8 acetone/CH_2Cl_2) gave the product as a brown solid (0.22 g, 1.90 mmol, 70%). ^{1}H NMR (500 MHz, $CDCl_3$, 298 K) δ: 8.22 (1H, dd, J = 2.2 Hz, 0.8 Hz, H_c), 7.53 (1H, dd, J = 8.6 Hz, 2.3 Hz, H_b), 6.46 (1H, dd, J = 8.6 Hz, 0.8 Hz, H_a), 4.69 (2H, br, H_{NH}), 3.06 (s, H_d). ^{13}C NMR (125 MHz, $CDCl_3$, 298 K) δ: 157.6, 151.6 (C_c), 141.0 (C_b), 108.7, 108.0 (C_a), 81.2, 77.8 (C_d). IR: ν (cm^{-1}) 3326, 3295, 3163, 2148, 1645, 1585, 1424, 1329, 1246, 1156. Anal. calcd for $C_7H_6N_2$·0.1 acetone: C, 70.74; H, 5.37; N, 22.60%. Found: C, 70.44; H, 5.17; N, 22.56%.

Synthesis of *N*-(5-((trimethylsilyl)ethynyl)pyridin-3-yl)acetamide (4). A glass tube containing diisopropylamine (7 mL) degassed with N_2 was charged with 5-bromopyridin-3-amine (500 mg, 2.89 mmol), CuI (55 mg, 0.29 mmol), Pd(dppf)$_2Cl_2$ (85 mg, 0.17 mmol) and TMS-acetylene (1.173 mL, 852 mg, 8.67 mmol) against a positive N_2 flow. The tube was sealed and stirred at 60 °C for 72 hours. 3 : 1 $CHCl_3$/IPA (100 mL) and aqueous 0.1 M EDTA/NH_4OH solution (100 mL) were added and the mixture stirred for one hour. The organic layer was washed with water (50 mL) and brine (50 mL), dried over Na_2SO_4, filtered, and the solvent was removed under vacuum. The resultant solid was purified by column chromatography (1 : 8 acetone/CH_2Cl_2) to give the product as a brown solid (512 mg, 2.71 mmol, 94%). ^{1}H NMR (500 MHz, $CDCl_3$, 298 K) δ: 8.10 (1H, d, J = 1.5 Hz, H_c), 8.01 (1H, d, J = 2.7 Hz, H_a), 7.04 (1H, dd, J = 2.7 Hz, 1.7 Hz, H_b), 0.25 (9H, s, H_d). ^{13}C NMR (125 MHz, $CDCl_3$, 298 K) δ: 142.9 (C_c), 141.9, 136.8 (C_a), 124.1 (C_b), 120.3, 101.9, 97.6, 0.0 (C_d). HR ESI-MS (MeOH) m/z = 191.10 $[M + H]^+$ (calc. for $C_{10}H_{15}N_2Si$, 191.10). Anal. calcd for $C_{10}H_{14}N_2OSi$: C, 63.11; H, 7.41; N, 14.62%; found: C, 63.40; H, 7.48; N, 14.62%. IR: ν (cm^{-1}) 3327, 3295, 3162, 2147, 1585, 1424, 1329, 1245.

Synthesis of 5-ethynylpyridin-3-amine (5). A solution of **4** (0.43 g, 2.3 mmol) in methanol (30 mL) with Na_2CO_3 (0.48 g, 4.5 mmol) was stirred at room temperature for 1 h. After filtration, the solvent was removed under vacuum, and the resultant solid was purified by column chromatography on silica (1 : 8 acetone/CH_2Cl_2) to give the product as a brown solid (0.25 g, 2.1 mmol, 96%). ^{1}H NMR (500 MHz, $CDCl_3$, 298 K) δ: 8.13 (1H, d, J = 2.7 Hz, H_c), 8.05 (1H, d, J = 2.7 Hz, H_a), 7.06 (1H, dd, J = 2.7 Hz, 2.7 Hz, H_b), 3.71 (2H, br, H_{NH}), 3.14 (1H, s, H_d). ^{13}C NMR (125 MHz, $CDCl_3$, 298 K) δ: 143.0 (C_c), 141.8, 137.1 (C_a), 124.0 (C_b), 119.1, 80.7, 79.8 (C_d). IR: ν (cm^{-1}) 3328, 3295, 3163, 3020, 2148, 1644, 1585, 1424, 1329, 1246. Anal. calcd for $C_7H_6N_2$·0.1 (acetone): C, 70.74; H, 5.37; N, 22.60%. Found: C, 70.96; H, 5.14; N, 22.80%. Mass spectral analysis was not successful for this compound.

Synthesis of tripy. A round bottom flask containing (2,6-dibromopyridin-4-yl)methanol (336 mg, 1.26 mmol), 3-ethynylpyridine (325 mg, 3.15 mmol), CuI (24 mg, 0.12 mmol) and Pd$(PPh_3)_2Cl_2$ (35 mg, 0.05 mmol) was purged with N_2, before addition of triethylamine (25 mL) and dry THF (25 mL). The reaction was stirred in the absence of light for 24 hours. CH_2Cl_2 (50 mL) and aqueous 0.1 M EDTA/NH_4OH solution (100 mL) were added and the mixture stirred at room temperature for 2 hours. After extraction into CH_2Cl_2 (2 × 100 mL), the combined organic layers were washed with brine (100 mL), dried over $MgSO_4$, and then filtered. The solvent was removed under vacuum. Column chromatography (2 : 3 CH_2Cl_2/acetone) gave the product as a colourless solid (280 mg, 0.90 mmol, 71%). ^{1}H NMR (500 MHz, CD_3CN, 298 K) δ: 8.81 (2H, dd, J = 2.1 Hz, 0.8 Hz, H_c), 8.61 (2H, dd, J = 4.9 Hz, 1.7 Hz, H_f), 7.98 (2H, ddd, J = 7.9 Hz, 2.2 Hz, 1.7 Hz, H_d), 7.58 (2H, t, J = 0.9 Hz, H_b), 7.41 (2H, ddd, J = 7.9 Hz, 4.9 Hz, 0.9 Hz, H_e), 4.67 (2H, dt, J = 5.9 Hz, 0.8 Hz, H_a), 3.55 (1H, t, J = 5.9 Hz, H_{OH}). ^{13}C NMR (500 MHz, CD_3CN, 298 K) δ: 154.1, 153.3 (C_c), 150.6 (C_f), 143.8, 139.9 (C_d), 125.3 (C_b), 124.4 (C_e), 119.9, 91.8, 86.2, 62.4 (C_a). HR ESI-MS (acetone) m/z = 645.21 $[2M + Na]^+$ (calc. for $C_{40}H_{26}N_6NaO_2$, 645.20), 334.10 $[M + Na]^+$ (calc. for $C_{20}H_{13}N_3NaO$, 334.10). IR: ν (cm^{-1}) 3204, 3032, 2923, 2213, 1685, 1596, 1547, 1475, 1415, 1189, 1076, 1023. Anal. calcd for $C_{20}H_{13}N_3O$·0.25 acetone: C, 76.48; H, 4.49; N, 12.90%. Found: C, 76.70; H, 4.49; N, 13.06%.

Synthesis of 2A-tripy. In a round bottom flask, diisopropylamine (20 mL) and THF (20 mL) were degassed with N_2, before addition of **3** (400 mg, 3.39 mmol), (2,6-dibromopyridin-4-yl) methanol (362 mg, 1.35 mmol), CuI (25 mg, 0.14 mmol), and Pd$(PPh_3)_2Cl_2$ (38 mg, 0.050 mmol) against a positive N_2 flow. The solution was heated at 50 °C for 48 hours. After removal of the solvent under vacuum, the resultant solid was taken up in 3 : 1 $CHCl_3$/IPA (150 mL) and aqueous 0.1 M EDTA/NH_4OH solution (50 mL) and stirred for 40 minutes. The organic layer was washed with brine, dried with Na_2SO_4, filtered and then the solvent was removed under vacuum. Purification of the resultant solid on a silica column deactivated with 3 : 97 triethylamine/CH_2Cl_2 (0.5/4.5/95 then 1/9/90 saturated aqueous NH_4OH solution/MeOH/CH_2Cl_2) gave the product as a brown solid (364 mg, 1.07 mmol, 79%). ^{1}H NMR (500 MHz, d_6-DMSO,

298 K) δ: 8.18 (2H, dd J = 2.3 Hz, 0.5 Hz, H_c), 7.57 (2H, dd, J = 8.6 Hz, 2.3 Hz, H_d), 7.42 (2H, s, H_b), 6.55 (4H, s, H_{NH}), 6.49 (2H, dd, J = 8.6 Hz, 0.6 Hz, H_e), 5.51 (1H, t, J = 5.8 Hz, H_{OH}), 4.54 (2H, d, J = 5.7 Hz, H_a). ^{13}C NMR (500 MHz, d_6-DMSO, 298 K) δ: 159.7, 153.0, 152.0 (C_c), 142.9, 139.7 (C_d), 122.6 (C_b), 107.7 (C_e), 104.9, 88.8, 88.0, 60.9 (C_a). HR ESI-MS (CH_3CN) m/z = 683.26 $[2M + H]^+$ (calc. for $C_{40}H_{31}N_{10}O_2$, 683.26), 342.13 $[M + H]^+$ (calc. for $C_{20}H_{16}N_5O$, 342.14). IR: ν (cm^{-1}) 3307, 3145, 2920, 2201, 1670, 1634, 1593, 1543, 1505, 1393, 1171, 1140, 1055, 1016. Anal. calcd for $C_{20}H_{15}N_5O{\cdot}CH_2Cl_2$: C, 69.00; H, 4.38; N, 20.02%. Found: C, 69.12; H, 4.51; N, 20.33%.

Synthesis of 3A-tripy. In a round bottom flask, diisopropylamine (20 mL) and THF (20 mL) were degassed with N_2, before **5** (365 mg, 3.09 mmol), (2,6-dibromopyridin-4-yl)methanol (275 mg, 1.03 mmol), CuI (20 mg, 0.10 mmol), and Pd $(PPh_3)_2Cl_2$ (36 mg, 0.05 mmol) were added against a positive N_2 flow. The solution was heated at 40 °C for 48 hours. After removal of the solvent under vacuum, the resultant solid was taken in 3 : 1 $CHCl_3$/IPA (150 mL) and aqueous 01. M EDTA/NH_4OH solution (50 mL) and stirred for 40 minutes. The organic layer was washed with brine (100 mL), dried with Na_2SO_4, filtered, and then the solvent was removed under vacuum. Purification of the resultant solid in a silica column deactivated with 3 : 97 triethylamine/CH_2Cl_2 (0.5/4.5/95 then 1/9/90 saturated aqueous NH_4OH solution/MeOH/CH_2Cl_2) gave the product as a brown solid (197 mg, 0.58 mmol, 56%). ^{1}H NMR (500 MHz, d_6-DMSO, 298 K) δ: 7.99 (2H, d, J = 2.9 Hz, H_e), 7.96 (2H, d, J = 1.6 Hz, H_c), 7.59 (2H, s, H_b), 7.09 (2H, t, J = 2.2 Hz, H_d), 5.60 (5H, m, H_{NH} & H_{OH}), 4.59 (2H, d, J = 5.8 Hz, H_a). ^{13}C NMR (125 MHz, d_6-DMSO, 298 K) δ: 153.6, 144.5, 142.2, 139.2 (C_c), 136.9 (C_e), 124.2 (C_b), 121.3 (C_d), 117.8, 89.8, 86.4, 60.8 (C_a). HR ESI-MS (CH_3CN) m/z = 340.1190 $[M + H]^+$ (calc. for $C_{20}H_{14}N_5O$, 340.1204). IR: ν (cm^{-1}) 3326, 3294, 3163, 3020, 2148, 1644, 1585, 1424, 1329, 1246, 1156. Anal. calcd for $C_{20}H_{15}N_5O$: C, 70.37; H, 4.43; N, 20.52%. Found: C, 70.21; H, 4.54; N, 20.52%.

Synthesis of $[Pd_2(tripy)_4](BF_4)_4$. A solution of **tripy** (62 mg, 0.20 mmol) and $[Pd(CH_3CN)_4](BF_4)_2$ (44 mg, 0.10 mmol) in acetonitrile (6 mL) was stirred for 1 hour. Vapor diffusion with diethyl ether gave a white solid (76 mg, 0.040 mmol, 85%). ^{1}H NMR (500 MHz, CD_3CN, 298 K) δ: 9.32 (8H, d, J = 1.8 Hz, H_c), 9.05 (8H, dd, J = 6.1 Hz, 1.1 Hz, H_f), 8.17 (8H, dt, J = 8.0 Hz, 1.4 Hz, H_d), 7.65 (8H, ddd, J = 8.0 Hz, 5.9 Hz, 0.6 Hz, H_e), 7.64 (8H, t, J = 0.8 Hz, H_b), 4.63 (8H, dd, J = 5.6 Hz, 0.8 Hz, H_a), 3.57 (4H, t, J = 5.6 Hz, H_{OH}). ^{13}C NMR (125 MHz, CD_3CN, 298 K) δ: 154.5, 154.4 (C_c), 151.4 (C_f), 144.5 (C_d), 143.2, 128.5 (C_e), 126.5 (C_b), 124.1, 94.8, 83.2, 62.2 (C_a). HR ESI-MS (CH_3CN) m/z = 816.1313 $[M - (BF_4)_2]^{2+}$ (calc. for $C_{80}H_{52}N_{12}O_4Pd_2$, 816.1313). IR: ν (cm^{-1}) 3211, 3097, 2976, 2921, 2852, 2220, 1685, 1595, 1545, 1483, 1420, 1043, 1027. Anal. calcd for $C_{80}H_{52}B_4F_{16}N_{12}O_4Pd_2{\cdot}3H_2O$: C, 51.67; H, 3.14; N, 9.04%. Found: C, 51.87; H, 3.09; N, 8.71%.

Synthesis of $[Pd_2(2A\text{-}tripy)_4](BF_4)_4$. A solution of **2A-tripy** (40 mg, 0.12 mmol) and $[Pd(CH_3CN)_4](BF_4)_4$ (26 mg, 0.060 mmol) in 1.5 mL d_6-DMSO in a tube was purged with N_2 and was heated at 50 °C for 6 hours. Diethyl ether (30 mL) was added and the solution shaken vigorously. After decanting the liquid portion, the precipitate was suspended in CH_2Cl_2 (5 mL) and isolated by filtration. After washing with CH_2Cl_2 (5 mL), the solid was dried under vacuum at 60 °C for 4 days to give the product as a red solid (32 mg, 0.017 mmol, 57%). ^{1}H NMR (500 MHz, d_6-DMSO, 298 K) δ: 8.77 (8H, d, J = 1.6 Hz, H_c), 8.11 (8H, s, H_{NH}), 7.84 (8H, dd, J = 8.9 Hz, 1.5 Hz, H_d), 7.56 (8H, s, H_b), 6.73 (8H, d, J = 8.9 Hz, H_e), 4.53 (8H, s, H_a). ^{13}C NMR (500 MHz, d_6-DMSO, 298 K) δ: 159.8, 153.5, 149.4 (C_c), 142.7 (C_d), 142.1, 125.3 (C_b), 112.6 (C_e), 107.7, 90.5, 84.6, 60.6 (C_a). ESI-MS (DMSO/CH_3CN) m/z = 394.60 $[M - 4(BF_4)]^{4+}$ (calc. for $C_{80}H_{60}N_{20}O_4Pd_2$, 394.58), 394.10 $[Pd(\mathbf{2A\text{-}tripy})_2]^{2+}$ (calc. for $C_{40}H_{30}N_{10}O_2Pd$, 394.08). IR: ν (cm^{-1}) 337, 3194, 2210, 1637, 1546, 1513, 1411, 1025. Anal. calcd for $C_{80}H_{60}B_4F_{16}N_{20}O_4Pd_2{\cdot}5H_2O{\cdot}4DMSO$: C, 45.50; H, 4.07; N, 12.03%. Found: C, 45.24; H, 3.78; N, 12.29%.

Synthesis of $[Pd_2(3A\text{-}tripy)_4](BF_4)_4$. A solution of **3A-tripy** (60 mg, 0.18 mmol) and $[Pd(CH_3CN)_4](BF_4)_4$ (39 mg, 0.090 mmol) in d_6-DMSO (0.75 mL) was sonicated for five minutes. Addition of ethyl acetate (20 mL)) resulted in precipitation of the product. The precipitate was collected by filtration, and washed with ethyl acetate (15 mL) and diethyl ether (15 mL) to give a brown solid (64 mg, 0.03 mmol, 75%). OR A solution of **3A-tripy** (60 mg, 0.18 mmol) and $[Pd(CH_3CN)_4](BF_4)_4$ (39 mg, 0.090 mmol) in DMF (2 mL) was sonicated for five minutes. Addition of ethyl acetate (20 mL) resulted in precipitation of the product. The precipitate was collected by filtration, and washed with ethyl acetate (15 mL) and diethyl ether (15 mL) to give a brown solid (60 mg, 0.03 mmol, 70%). ^{1}H NMR (500 MHz, d_6-DMSO, 298 K) δ: 8.36 (8H, s, H_e), 8.26 (8H, s, H_c), 7.63 (8H, s, H_b), 7.30 (2H, s, H_d), 6.41 (8H, s, H_{NH}), 5.59 (4H, br, H_{OH}), 4.55 (8H, s, H_a). ^{13}C NMR (125 MHz, d_6-DMSO, 298 K) δ: 154.0, 146.9, 141.4, 138.3 (C_c), 135.9 (C_e), 125.3 (C_d), 125.1 (C_b), 120.7, 119.1, 91.9, 83.3, 60.7 (C_a). HR ESI-MS (DMSO/CH_3CN) m/z = 394.5820 $[M - 4(BF_4)_4]^{4+}$ (calc. for $C_{80}H_{60}N_{20}O_4$, 394.5797), 342.1401 $[\mathbf{3A\text{-}tripy} + H]^+$ (calc. for $C_{20}H_{16}N_5O$, 342.1401). IR: ν (cm^{-1}) 3468, 3384, 3230, 2220, 1637, 1592, 1547, 1443, 1020. Anal. calcd for $C_{80}H_{60}B_4F_{16}N_{20}O_4Pd_2{\cdot}5H_2O{\cdot}4DMSO$: C, 45.50; H, 4.07; N, 12.03%. Found: C, 45.20; H, 3.77; N, 12.28%.

X-ray crystallography $[Pd_2(2A\text{-}tripy)_4](BF_4)_4$

Yellow block crystals of $[Pd_2(\mathbf{2A\text{-}tripy})_4](BF_4)_4$ were grown by vapour diffusion of diethyl ether in a solution of MeCN. X-ray data were collected at 100(1) K on an Agilent Technologies Supernova system using Cu Kα radiation with exposures over 1.0°, and data were treated using CrysAlisPro[28] software. The structure was solved using Sir-97 [29] and weighted full-matrix refinement on F^2 was carried out using SHELXL-97 [30] running within the WinGX package.[31] All non-hydrogen atoms were refined anisotropically. Hydrogen atoms were placed in calculated positions and refined using a riding model. The structure was solved in the primitive tetragonal space group $P4/m$ and refined to an R_1 value of 14.4%. The asymmetric unit contains two half ligands and two quarter occupancy palladium ions. The counter-anions and solvent molecules present in the

solvent lattice were severely disordered and could not be appropriately modelled. The SQUEEZE routine within PLATON was employed to resolve this problem, resulting in ten void spaces (total of 460 electrons), variously assigned to tetrafluoroborate anions (8 in total), H_2O (5 in total) and MeCN (3 in total) solvent molecules (total of 444 electrons), as described below. Despite repeated efforts (>50 crystallisations and data collections over a two year period) to crystallise the compound, the most suitable candidate was small and a poor diffractor. The data quality is poor, with two A alerts (a large Hirshfield difference and high MainMol $U_{eq.}$ compared to neighbours) and many B alerts, and we emphasise that metric data cannot be reliably extracted from the structure and should be treated with caution. However, the connectivity of the cationic framework is readily apparent. The methylene alcohol substituents from the four neighbouring cages in the lattice interpenetrate the cavity of each cage (Fig. 3 and ESI†), interpenetrating groups shown in spacefilling mode (yellow, green, blue and pink) and preclude cisplatin encapsulation in the solid state. Around the coordinating pyridine rings, the amino groups form a hydrogen bonding network. SQUEEZE details and crystallographic parameters can be found in the ESI.†

Acknowledgements

The authors wish to thank Dr Dave McMorran and Dr Warrick Lo for fruitful discussions, and Christopher Anderson for early synthetic efforts. DP and JEML thank the University of Otago for PhD scholarships. JDC (Laurenson Award, LA307) and DP (MacQueen Summer Scholarship) thank the Otago Medical Research Fund for financial support. The authors thank the Department of Pharmacology and Toxicology and the Department of Chemistry, University of Otago for additional funding.

Notes and references

1 (*a*) For some selected recent reviews see: (*b*) T. R. Cook and P. J. Stang, *Chem. Rev.*, 2015, **115**, 7001–7045; (*c*) A. M. Castilla, W. J. Ramsay and J. R. Nitschke, *Acc. Chem. Res.*, 2014, **47**, 2063–2073; (*d*) M. M. J. Smulders, I. A. Riddell, C. Browne and J. R. Nitschke, *Chem. Soc. Rev.*, 2013, **42**, 1728–1754; (*e*) N. J. Young and B. P. Hay, *Chem. Commun.*, 2013, **49**, 1354–1379; (*f*) T. Nakamura, H. Ube and M. Shionoya, *Chem. Lett.*, 2013, **42**, 328–334; (*g*) J. E. Beves, B. A. Blight, C. J. Campbell, D. A. Leigh and R. T. McBurney, *Angew. Chem., Int. Ed.*, 2011, **50**, 9260–9327; (*h*) R. Chakrabarty, P. S. Mukherjee and P. J. Stang, *Chem. Rev.*, 2011, **111**, 6810–6918; (*i*) Y.-F. Han, H. Li and G.-X. Jin, *Chem. Commun.*, 2010, **46**, 6879–6890; (*j*) M. D. Ward, *Chem. Commun.*, 2009, 4487–4499; (*k*) C. R. K. Glasson, L. F. Lindoy and G. V. Meehan, *Coord. Chem. Rev.*, 2008, **252**, 940–963; (*l*) M. Han, D. M. Engelhard and G. H. Clever, *Chem. Soc. Rev.*, 2014, **43**, 1848–1860; (*m*) N. B. Debata, D. Tripathy and D. K. Chand, *Coord. Chem. Rev.*, 2012, **256**, 1831–1945.

2 (*a*) M. Yoshizawa and M. Fujita, *Bull. Chem. Soc. Jpn.*, 2010, **83**, 609–618; (*b*) M. Yoshizawa, J. K. Klosterman and M. Fujita, *Angew. Chem., Int. Ed.*, 2009, **48**, 3418–3438.

3 (*a*) C. J. Brown, F. D. Toste, R. G. Bergman and K. N. Raymond, *Chem. Rev.*, 2015, **115**, 3012–3035; (*b*) S. H. A. M. Leenders, R. Gramage-Doria, B. de Bruin and J. N. H. Reek, *Chem. Soc. Rev.*, 2015, **44**, 433–448; (*c*) A. M. Lifschitz, M. S. Rosen, C. M. McGuirk and C. A. Mirkin, *J. Am. Chem. Soc.*, 2015, **137**, 7252–7261; (*d*) M. J. Wiester, P. A. Ulmann and C. A. Mirkin, *Angew. Chem., Int. Ed.*, 2011, **50**, 114–137.

4 (*a*) B. Therrien, *CrystEngComm*, 2015, **17**, 484–491; (*b*) B. Therrien, *Chem. – Eur. J.*, 2013, **19**, 8378–8386; (*c*) J. W. Yi, N. P. E. Barry, M. A. Furrer, O. Zava, P. J. Dyson, B. Therrien and B. H. Kim, *Bioconjugate Chem.*, 2012, **23**, 461–471; (*d*) B. Therrien, *Top. Curr. Chem.*, 2012, **319**, 35–56; (*e*) F. Schmitt, J. Freudenreich, N. P. E. Barry, L. Juillerat-Jeanneret, G. Suss-Fink and B. Therrien, *J. Am. Chem. Soc.*, 2012, **134**, 754–757; (*f*) O. Zava, J. Mattsson, B. Therrien and P. J. Dyson, *Chem. – Eur. J.*, 2010, **16**, 1428–1431; (*g*) B. Therrien, G. Suess-Fink, P. Govindaswamy, A. K. Renfrew and P. J. Dyson, *Angew. Chem., Int. Ed.*, 2008, **47**, 3773–3776; (*h*) Y.-R. Zheng, K. Suntharalingam, T. C. Johnstone and S. J. Lippard, *Chem. Sci.*, 2015, **6**, 1189–1193.

5 (*a*) P. Mal, B. Breiner, K. Rissanen and J. R. Nitschke, *Science*, 2009, **324**, 1697–1699; (*b*) M. Yamashina, Y. Sei, M. Akita and M. Yoshizawa, *Nat. Commun.*, 2014, 5.

6 (*a*) V. Blanco, M. D. Garcia, A. Terenzi, E. Pia, A. Fernandez-Mato, C. Peinador and J. M. Quintela, *Chem. – Eur. J.*, 2010, **16**, 12373–12380; (*b*) I. A. Riddell, M. M. J. Smulders, J. K. Clegg and J. R. Nitschke, *Chem. Commun.*, 2011, **47**, 457–459.

7 (*a*) R. A. Kaner and P. Scott, *Future Med. Chem.*, 2015, **7**, 1–4; (*b*) T. R. Cook, V. Vajpayee, M. H. Lee, P. J. Stang and K.-W. Chi, *Acc. Chem. Res.*, 2013, **46**, 2464–2474.

8 (*a*) L. Xu, Y.-X. Wang and H.-B. Yang, *Dalton Trans.*, 2015, **44**, 867–890; (*b*) O. Chepelin, J. Ujma, X. Wu, A. M. Z. Slawin, M. B. Pitak, S. J. Coles, J. Michel, A. C. Jones, P. E. Barran and P. J. Lusby, *J. Am. Chem. Soc.*, 2012, **134**, 19334–19337; (*c*) M. Han, R. Michel, B. He, Y.-S. Chen, D. Stalke, M. John and G. H. Clever, *Angew. Chem., Int. Ed.*, 2013, **52**, 1319–1323.

9 (*a*) R. J. Archer, C. S. Hawes, G. N. L. Jameson, V. McKee, B. Moubaraki, N. F. Chilton, K. S. Murray, W. Schmitt and P. E. Kruger, *Dalton Trans.*, 2011, **40**, 12368–12373; (*b*) A. Ferguson, M. A. Squire, D. Siretanu, D. Mitcov, C. Mathoniere, R. Clerac and P. E. Kruger, *Chem. Commun.*, 2013, **49**, 1597–1599; (*c*) R. A. Bilbeisi, S. Zarra, H. L. C. Feltham, G. N. L. Jameson, J. K. Clegg, S. Brooker and J. R. Nitschke, *Chem. – Eur. J.*, 2013, **19**, 8058–8062.

10 (*a*) V. Croue, S. Goeb and M. Salle, *Chem. Commun.*, 2015, **51**, 7275–7289; (*b*) M. Frank, J. Hey, I. Balcioglu, Y.-S. Chen,

D. Stalke, T. Suenobu, S. Fukuzumi, H. Frauendorf and G. H. Clever, *Angew. Chem., Int. Ed.*, 2013, **52**, 10102–10106.

11 (*a*) S. M. McNeill, D. Preston, J. E. M. Lewis, A. Robert, K. Knerr-Rupp, D. O. Graham, J. R. Wright, G. I. Giles and J. D. Crowley, *Dalton Trans.*, 2015, **44**, 11129–11136; (*b*) S. V. Kumar, W. K. C. Lo, H. J. L. Brooks and J. D. Crowley, *Inorg. Chim. Acta*, 2015, **425**, 1–6; (*c*) S. K. Vellas, J. E. M. Lewis, M. Shankar, A. Sagatova, J. D. A. Tyndall, B. C. Monk, C. M. Fitchett, L. R. Hanton and J. D. Crowley, *Molecules*, 2013, **18**, 6383–6407; (*d*) J. E. M. Lewis, E. L. Gavey, S. A. Cameron and J. D. Crowley, *Chem. Sci.*, 2012, **3**, 778–784.

12 D. Preston, A. Fox-Charles, W. K. C. Lo and J. D. Crowley, *Chem. Commun.*, 2015, **51**, 9042–9045.

13 (*a*) Other workers have also shown that nucleophiles will react with palladium(II) based metallosupramolecular cages, see: (*b*) R. Zhu, J. Luebben, B. Dittrich and G. H. Clever, *Angew. Chem., Int. Ed.*, 2015, **54**, 2796–2800; (*c*) J. J. Henkelis, J. Fisher, S. L. Warriner and M. J. Hardie, *Chem. – Eur. J.*, 2014, **20**, 4117–4125.

14 (*a*) A. M. Johnson, O. Moshe, A. S. Gamboa, B. W. Langloss, J. F. K. Limtiaco, C. K. Larive and R. J. Hooley, *Inorg. Chem.*, 2011, **50**, 9430–9442; (*b*) P. Liao, B. W. Langloss, A. M. Johnson, E. R. Knudsen, F. S. Tham, R. R. Julian and R. J. Hooley, *Chem. Commun.*, 2010, **46**, 4932–4934; (*c*) K. J. Kilpin, M. L. Gower, S. G. Telfer, G. B. Jameson and J. D. Crowley, *Inorg. Chem.*, 2011, **50**, 1123–1134.

15 (*a*) Other workers have previously shown that 2-aminopyridine ligands will coordinate to palladium(II) and platinum (II) ions through the pyridyl nitrogen in a monodentate fashion, see ref. 15*b*–*d*. However, the 2-aminopyridine unit can also act as a bridging ligand, see ref. 15*e*; (*b*) K. Sakai, N. Akiyama and M. Mizota, *Acta Crystallogr., Sect. E: Struct. Rep. Online*, 2003, **59**, m459–m461; (*c*) C. Gómez-Vaamonde, A. Alvarez-Valdés, M. Navarro-Ranninger and J. Masaguer, *Transition Met. Chem.*, 1984, **9**, 52–54; (*d*) S. A. Al-Jibori, Q. K. A. Al-Jibori, H. Schmidt, K. Merzweiler, C. Wagner and G. Hogarth, *Inorg. Chim. Acta*, 2013, **402**, 69–74; (*e*) J. M. Casas, B. E. Diosdado, J. Forniés, A. Martín, A. J. Rueda and A. G. Orpen, *Inorg. Chem.*, 2008, **47**, 8767–8775.

16 (*a*) While our manuscript was being refereed Casini, Kuhn and co-workers reported the X-ray crystal structure of the cisplatin–$[Pd_2(\mathbf{tripy})_4]^{4+}$ host guest adduct, see: (*b*) A. Schmidt, V. Molano, M. Hollering, A. Pöthig, A. Casini and F. E. Kühn, *Chem. – Eur. J.*, 2016, **22**, 2253–2256.

17 W. M. Haynes, *CRC Handbook of Chemistry and Physics*, Taylor & Francis, 93rd edn, 2012.

18 (*a*) Huynh and co-workers have shown that benzimidazol-2-ylidene-dibromopalladium(II) complexes can be used to probe the σ-donor strength of the ligands *trans* to the benzimidazol-2-ylidene. They have found that there is a direct relationship between the σ-donor strength of the *trans* monodentate ligand and the chemical shift of the benzimidazole carbene carbon in the ^{13}C NMR spectra of the dibromopalladium(II) complexes, see: (*b*) H. V. Huynh, Y. Han, R. Jothibasu and J. A. Yang, *Organometallics*, 2009, **28**, 5395–5404.

19 (*a*) J. E. M. Lewis, A. B. S. Elliott, C. J. McAdam, K. C. Gordon and J. D. Crowley, *Chem. Sci.*, 2014, **5**, 1833–1843; (*b*) J. E. M. Lewis, C. J. McAdam, M. G. Gardiner and J. D. Crowley, *Chem. Commun.*, 2013, **49**, 3398–3400.

20 Cisplatin binding within the $[Pd_2(\mathbf{tripy})_4]^{4+}$ cage cavity is only observed in CD_3CN and DMF-d_7. We have generated a water soluble $[Pd_2(\mathbf{tripy})_4]^{4+}$ cage using nitrate (NO_3^-) counter anions and examined the binding of cisplatin in D_2O (ESI†). As we have seen previously in D_2O (ref. 19*a*) no host–guest interaction between the cage and cisplatin was observed (ESI†). Similarly, we have also examined the host–guest interaction between the$[Pd_2(\mathbf{tripy})_4]^{4+}$ cage and cisplatin in DMSO-d_6 (ESI†). As with the D_2O experiments no interaction between the cage and the cisplatin was observed. Additionally, the DMSO solvent reacts with cisplatin releasing either (Cl^- or NH_3) ligands which then react with the $[Pd_2(\mathbf{tripy})_4]^{4+}$ cation leading to cage decomposition (ESI†).

21 T. Y. Kim, N. T. Lucas and J. D. Crowley, *Supramol. Chem.*, 2015, **27**, 734–745.

22 A referee suggested that the hydrogen bonding between the *exo*-methylene alcohol unit and the central *endo*-pyridyl group observed in the crystal structure of $[Pd_2(\mathbf{2A\text{-}tripy})_4]^{4+}$ could be responsible for the lack of cisplatin binding. We rule that postulate out for the following reasons: (1) ^1H NMR and DOSY experiments (DMF-d_7, ESI†) suggest that the $[Pd_2(\mathbf{2A\text{-}tripy})_4]^{4+}$ cage is monomeric in solution. The diffusion coefficient for the $[Pd_2(\mathbf{2A\text{-}tripy})_4]^{4+}$ cage was essentially identical to that of cage that does not feature the *exo*-methylene alcohol unit suggesting that those two cages are of very similar size in solution. Additionally, the ^1H NMR spectra of the cage are not concentration dependant ruling out any aggregation of the $[Pd_2(\mathbf{2A\text{-}tripy})_4]^{4+}$ cage into a larger oligomeric or polymeric architectures; (2) All the cages studied have the *exo*-methylene alcohol unit and the central *endo*-pyridyl group. Thus if hydrogen bonding between those substituents was a factor it would be expected to interfere with cisplatin binding in all the cage systems. It does not, the $[Pd_2(\mathbf{3A\text{-}tripy})_4]^{4+}$ and $[Pd_2(\mathbf{tripy})_4]^{4+}$ both interact with cisplatin in DMF solution.

23 A. Ahmedova, D. Momekova, M. Yamashina, P. Shestakova, G. Momekov, M. Akita and M. Yoshizawa, *Chem. – Asian J.*, 2016, **11**, 474–477.

24 W. K. C. Lo, G. S. Huff, D. Preston, D. A. McMorran, G. I. Giles, K. C. Gordon and J. D. Crowley, *Inorg. Chem.*, 2015, **54**, 6671–6673.

25 P. R. Symmers, M. J. Burke, D. P. August, P. I. T. Thomson, G. S. Nichol, M. R. Warren, C. J. Campbell and P. J. Lusby, *Chem. Sci.*, 2015, **6**, 756–760.

26 C. M. Amb and S. C. Rasmussen, *J. Org. Chem.*, 2006, **71**, 4696–4699.

27 H. V. Huynh, Y. Han, J. H. H. Ho and G. K. Tan, *Organometallics*, 2006, **25**, 3267–3274.

28 *CrysAlisPro*, Agilent Technologies, Yarnton, England, 2012.
29 A. Altomare, M. C. Burla, M. Camalli, G. L. Cascarano, C. Giacovazzo, A. Guagliardi, A. G. G. Moliterni, G. Polidori and R. Spagna, *J. Appl. Crystallogr.*, 1999, **32**, 115–119.
30 G. Sheldrick, *Acta Crystallogr., Sect. A: Found. Crystallogr.*, 2008, **64**, 112–122.
31 L. Farrugia, *J. Appl. Crystallogr.*, 1999, **32**, 837–838.